Measuring Time-Averaged and Dynamic Surface Pressures on Passenger Car Wheels Using Fast-Response PSP

Jan Marcel Hübner, Dr. Sven Lange, Mathias Hähnel, Dr. Michael Hilfer

Aerodynamics Development
Volkswagen AG
Berliner Ring 2, 38440 Wolfsburg

Institute of Fluid Mechanics
Technische Universität Braunschweig
Hermann-Blenk-Straße 37, 38108 Braunschweig

jan.marcel.huebner@volkswagen.de
sven.lange5@volkswagen.de
mathias.haehnel@volkswagen.de
michael.hilfer@tu-braunschweig.de

Abstract

To enhance passenger car efficiency, reducing aerodynamic drag is crucial, with a significant portion of the drag arising from rotating wheels. Understanding surface pressures on a wheel rim, an area still largely unexplored, is essential for effective development of wheel-related measures. This paper introduces a method for measuring surface pressure on a wheel rim and adjacent body areas both across the whole area and transiently during driving and wind tunnel tests using Fast-Response Pressure Sensitive Paint (PSP). The experimental setup is detailed, covering components, paint characterization, the calibration method using pressure taps, and initial wind tunnel tests at 140 kph using a Volkswagen ID.7 production vehicle with stationary wheels. Measurements are conducted with a high-speed camera at 4000 fps using the intensity-based method with a continuous light source. Results include time-averaged and frequency information, demonstrating the method's capability to capture dynamic pressure distributions. Compared to traditional techniques, PSP offers significant advantages such as high spatial resolution and the elimination of the need for sensors on fast-rotating parts. These findings open new possibilities for understanding flow dynamics around tires, also providing valuable information for improving Computational Fluid Dynamics (CFD) simulations and ground simulation in wind tunnels. Future measurements will focus on rotating wheels in wind tunnel and on-road tests.

Contribution: 2025 FKFS Conference on Vehicle Aerodynamics and Thermal Management
15 – 16 October 2025 | Leinfelden-Echterdingen

1 Introduction

In the automotive industry, increasing environmental awareness, growing demand for electric vehicles with extended range, and stricter regulatory requirements have shifted the focus towards improving vehicle efficiency, particularly by reducing aerodynamic drag coefficients. Since the airflow around the wheels accounts for approximately $20 - 30\ \%$ of the aerodynamic drag of an electric vehicle [1], there is a strong emphasis on gaining a deeper understanding of the flow phenomena around wheels and wheel housings. Due to the rotation and complex geometries (tire tread, rim), accurately capturing these flow phenomena is a complex measurement challenge. Additionally, replicating road-like flow conditions around the wheels in wind tunnels is difficult, especially near the ground. Modern automotive wind tunnels are therefore typically equipped with five-belt systems that simulate ground movement and wheel rotation.

This paper aims to establish a foundation for measuring surface pressures on wheels and adjacent body areas both on the road and in the wind tunnel. The goal is to gain deeper insights into the flow structures around the wheels and to evaluate how closely ground simulation in wind tunnels replicates real road conditions.

Previous studies [2] have for example identified frequencies in the vehicle wake that are attributed to the interaction between wheel rotation and the number of rim spokes. Numerous other works have focused on measuring flow fields around wheels in wind tunnels [1, 3, 4]. These studies revealed that wind tunnel ground simulation, for example through gap flows, influences flow structures around the wheels. However, to the authors' knowledge, surface pressures on rotating rims have not yet been measured, an approach that could provide even deeper insights into the flow field.

To address this gap and achieve a more precise understanding of the flow around rims, this study focuses on developing a measurement methodology capable of capturing high-resolution, time-resolved surface pressures on rims and surrounding body areas. Hilfer [5] demonstrated that pressure fluctuations can be measured on rotating geometries using pressure-sensitive paint. This technique is now being applied to passenger car wheels. Additionally, PSP was previously explored in automotive applications [6], finding it to be a very useful tool for flow diagnostics with an accuracy of $\pm\ 0.2\ c_\mathrm{p}$ (at high dynamic pressures between 1914 Pa and 2872 Pa). It is indicated, that for lower dynamic pressures, only qualitative measurements can be conducted. In collaboration with the Institute of Fluid Mechanics at TU Braunschweig, papers by Gregory [7] and Kasai [8] were identified, describing a paint capable of resolving small pressure differences of 30 Pa per brightness level and performing high-frequency measurements up to 2.2 kHz using a 12 bit high-speed camera. Building on that, it is the goal to be able to conduct quantitative measurements also for dynamic pressures around 930 Pa, corresponding to a freestream velocity of 140 kph. Based on simulation results indicating expected pressure ranges between -1200 Pa and 200 Pa in the wheel area, this paint was selected. The basis for the setup used in this work was laid in the master's thesis of Andreas Sieling [9].

Contribution: 2025 FKFS Conference on Vehicle Aerodynamics and Thermal Management
15 – 16 October 2025 | Leinfelden-Echterdingen

2 Development of the Measurement Setup

The development of the setup for pressure-sensitive paint (PSP) measurements focused on ensuring usability both in wind tunnel and on-road tests, while delivering comparable data across both environments. Additionally, the setup should allow measurements at both the front and rear axles.

The measurement setup for PSP includes the paint itself, a high-speed camera, and UV LED spotlights. Both the camera and the UV LEDs must be directed at the surface coated with PSP. Accordingly, a setup was developed that enables both the high-speed camera and UV LED spotlights to be aimed at the wheel rim and adjacent body areas. The development process of this setup is described in the following sections.

2.1 Test Vehicle and Test Facility

The test vehicle used is a Volkswagen ID.7 (see Figure 1). The vehicle is equipped with 19-inch wheels. For the principle tests described in this paper, a 4 mm thick carbon disc was mounted on the front left rim to simplify the geometry.

Figure 1: ID.7 in the AAK.

The experimental investigations were conducted in the Aerodynamics-Aeroacoustics Wind Tunnel (AAK) located in Wolfsburg. The facility is a Göttingen-type aerodynamic wind tunnel specifically designed for full-scale vehicle testing. It features an open test section with a rectangular nozzle cross-section measuring $6.2\ \text{m} \times 3.86\ \text{m}$, corresponding to a cross-sectional area of $23.87\ \text{m}^2$. The maximum flow velocity used during the experiments was 140 kph, which corresponds to a Reynolds number of approximately 1.31×10^7 for a vehicle length of 4.96 m. The flow quality in the measurement section is characterized by a turbulence intensity of less than 0.2 % [10].

To realistically simulate road conditions, the wind tunnel is equipped with a 5-belt system. The central main belt (CMB) beneath the vehicle replicates the relative movement of the road, while four additional wheel drive units (WDU) under each wheel enable correct wheel rotation. Measurements were carried out at a constant air temperature of 22 °C and an ambient pressure of 101007 hPa.

2.2 Measurement Setup Concept

The measurement setup is designed to enable data acquisition at both the front and rear axles. Additionally, it aims to capture flow information upstream and downstream of the wheel, as well as directly on the rim surface. The basic concept of a setup that fulfills these requirements is illustrated schematically for the front axle in Figure 2. The same configuration is intended to be used at the rear axle as well, although the measurements in this study are exclusively conducted at the front axle.

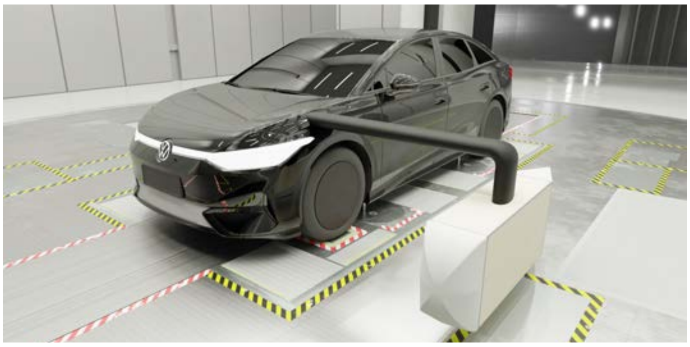

Figure 2: Concept of the measurement setup enabling PSP testing on the road.

The illustrated concept consists of a modular structure comprising a support wing and a measurement pod, allowing for quick installation and removal. The setup can be mounted either in the engine compartment or behind the rear seat. The measurement pod is designed to house both the UV LED spotlights and the high-speed camera. To minimize the frontal area of the pod, the camera is installed longitudinally, and its field of view is redirected via a mirror.

2.3 Design of Support Arm and Measurement Pod

Several factors were considered when determining the distance between the measurement pod and the vehicle, particularly the influence on the airflow around the wheels, which decreases with increasing distance to the vehicle, as well as the torque acting on the vehicle and the measurement pod's proximity to the shear layer of the wind tunnel. In its final configuration, the distance is set to 1100 mm. To minimize aerodynamic interference and reduce vibrations in the measurement pod and support arm, both components were covered with streamlined bodies.

The aerodynamic influence of the setup was also evaluated using CFD simulations (see Figure 3). The results show that while the setup does affect the static pressure field on the vehicle and the rim, especially around the support wing, the pressure difference on the rim and in the upstream and downstream regions is altered by a maximum of $\Delta c_\mathrm{p} = \pm 0.02$.

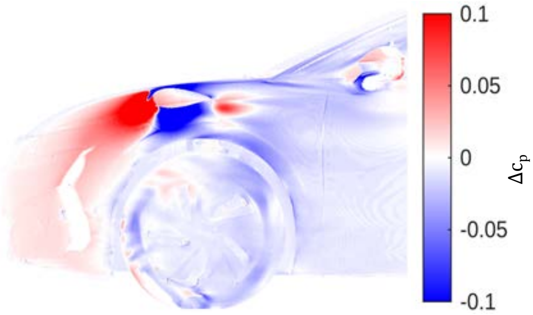

Figure 3: Difference in Δc_p between a CFD simulation with and without the support wing and measurement pod.

2.4 Optics

Inside the measurement pod, the camera and its optics are installed. The camera records at 4000 fps with an exposure time of 247 µs and a 12 bit resolution (4096 brightness levels). Accordingly, one brightness level corresponds to a normalized intensity of 2.44×10^{-4}. Combined with the paint's pressure sensitivity of 0.08 % / 100 Pa, this results in a pressure resolution of approximately 30 Pa per brightness level of the camera. A bandpass filter with a peak transmission at 650 nm is mounted in front of the lens. This ensures that the camera captures only the light emitted by the paint (650 nm). To ensure that the light illuminating the paint originates solely from the LED spotlights (395 nm), bandpass filter glasses are also placed in front of the spotlights, selected for peak transmission at 395 nm.

2.5 Spotlights

For the UV LED spotlights aimed at the measurement area, key requirements include sufficient light output, uniform illumination, and consistent light quality to prevent interference frequencies from being captured by the camera, which could negatively influence unsteady measurement results. To ensure adequate lighting and uniform coverage, four spotlights are positioned to illuminate the measurement area. During reference recordings, where only the UV LED spotlights are active, a frequency analysis using FFT was performed to assess the influence of the spotlights on the measurement results. The resulting amplitudes are plotted against their corresponding frequencies in Figure 4. The analysis shows that the baseline noise generated by the

LED spotlights is below 0.5×10^{-4}, which is five times lower than the resolution threshold (red line in Figure 4).

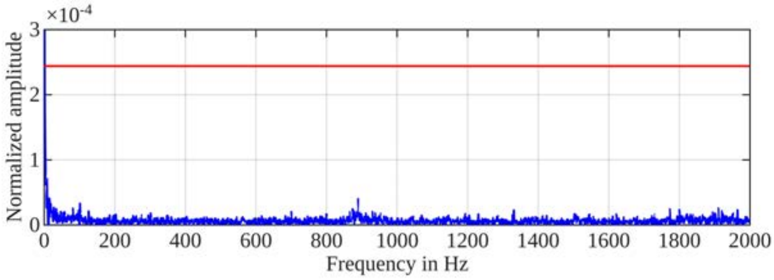

Figure 4: FFT analysis of the UV LED spotlights during a reference measurement. Red line marks normalized intensity of one camera brightness level.

2.6 Wall Pressure Taps

To calibrate the PSP measurements, which only provide relative pressure changes, against absolute values, wall pressure taps are distributed across the wheel arch. The pressure taps, each with a diameter of 0.8 mm, are connected to the pressure measurement system via vinyl tubing.

2.7 Complete Setup

All these components were assembled for the measurements. The complete setup is shown in Figure 5.

Figure 5: ID.7 in the AAK including measurement equipment.

In the right image, the Plexiglas window through which the camera views the measurement area is visible in the center of the pod. Surrounding the window are the four UV LED spotlights. When these are switched on and the wind tunnel lighting is turned off, the setup appears as shown in Figure 6.

Figure 6: Setup in the AAK with activated UV LED spotlights.

3 Experimental Method

The following section describes the experimental procedure for conducting and evaluating the measurements. First, the test sequence is outlined, followed by the methodology used to analyze the PSP measurements.

3.1 Test Procedure

Once the vehicle is positioned in the wind tunnel as shown in Figure 5, the procedure is as follows: After the airflow velocity reaches 140 kph, pressure measurements via wall pressure taps are initiated, the LED spotlights are switched on, and the camera is triggered to record the measurement (4000 fps, 247 µs exposure time, 4096 frames). After recording, the LED spotlights are turned off and the pressure measurement via taps is stopped. The acquired frames are then saved. It must also be ensured that a reference measurement is recorded under known ambient conditions, which allows the actual frames to be corrected for disturbances such as uneven illumination. For the scope of this paper, all measurements are conducted with stationary wheels.

3.2 Evaluation Method for Pressure-Sensitive Paint

A representative raw image from a recorded measurement is shown in Figure 7. It illustrates that the camera captures only the light emitted from the painted surface, as intended. The following describes the methodology for converting the measurement data into a time-averaged pressure field, followed by the approach used to evaluate initial unsteady results.

Figure 7: Raw image from the PSP measurement.

To obtain the time-averaged pressure field, all frames are aligned, so there is no frame-to-frame movement. Then, both the measurement and reference frames are time-averaged and the measurement is normalized, resulting in a normalized intensity distribution. This distribution is scaled using the time-averaged values from the wall pressure taps (in situ and interea calibration), producing a spatially resolved, time-averaged pressure field. To extract unsteady pressure information, each frame of the measurement is normalized individually. The entire frame-wise normalized measurement is then analyzed using FFT (Fast Fourier Transform). This yields frequency maps, which can be evaluated for each frequency of interest (up to 2000 Hz at 4000 fps). These maps allow the identification of vortex footprints via regions of elevated amplitude, and the assignment of corresponding frequencies to the vortices.

4 Results and Analysis

The following section presents and analyzes the results obtained from the PSP measurements. For scaling and validation purposes, the time-averaged pressures from the wall pressure taps are used. Additionally, simulations (Volkswagen standard setup [11]) are conducted to compare with the experimental results. These simulations are briefly described below.

4.1 CFD-Simulation

In Figure 8 a), the separation zones around the ID.7, including the measurement setup, are identified via CFD simulation. Notable features include the separation at the air curtain (1), the tire wake vortex (2), vortices detaching at the wheel spoiler (3) and (4), and vortices occurring in the upper region of the wheel and wheel housing (5) and (6). In the time-averaged static pressure field shown in Figure 8 b), the footprints of vortices (2), (4), (6), and (7) are particularly visible. These will now be compared with the PSP measurements.

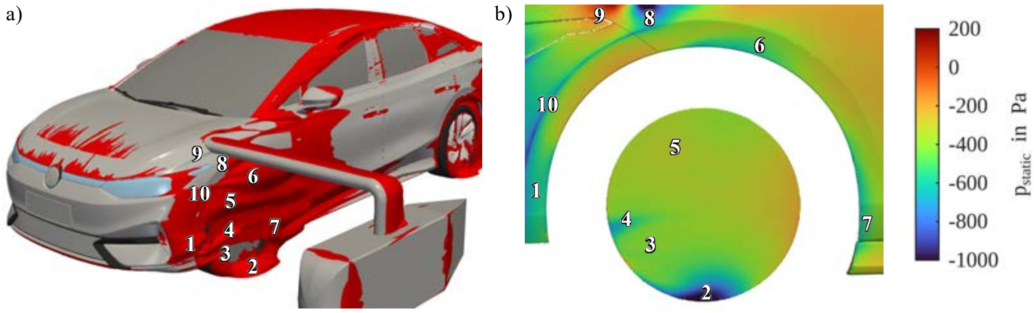

Figure 8: a) Separation zones around the ID.7 with stationary wheels and discs mounted on the rims. b) Static pressure field (both CFD simulations).

4.2 PSP Measurements

The evaluation of the PSP measurements is divided into time-averaged (steady) and unsteady results. The analysis of the time-averaged images follows the procedure described in Section 3.2. The normalized intensity field is scaled using the pressure values from the wall pressure taps. The linear fit used for this scaling is shown in Figure 9, indicating a pressure sensitivity of 0.17 % / 100 Pa. This implies that one brightness level of the camera corresponds to a pressure change of approximately 15 Pa.

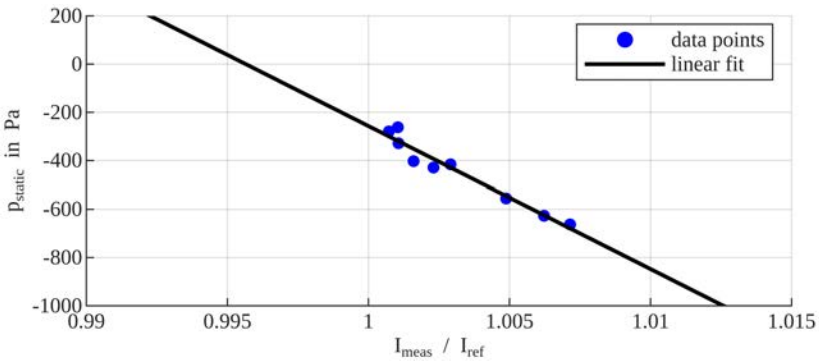

Figure 9 : Linear fit between the static pressure from wall pressure tap measurements and the corresponding normalized light intensity.

The resulting time-averaged static pressure field is shown in Figure 10, with the wall pressure tap values marked (black-bordered points). It is evident that the pressure field measured via PSP closely matches the values obtained from the wall pressure taps. The maximum deviation between a tap and its corresponding PSP value is approximately 50 Pa, which corresponds to a Δc_{p} of about 0.05.

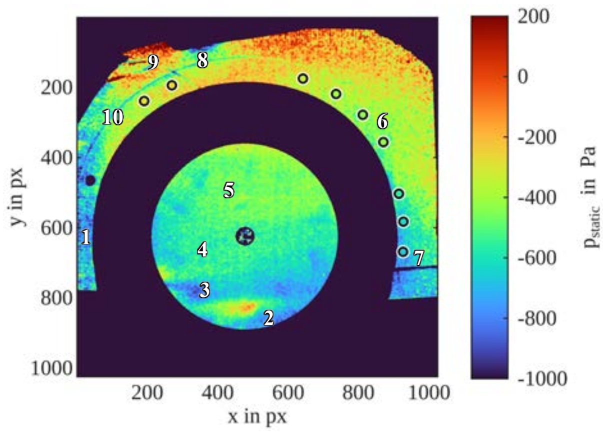

Figure 10: Time-averaged, static pressure field from the pressure-sensitive paint measurement.

When compared to the pressure field from the CFD simulation, key features such as the acceleration of the flow around the wing profile in the upper image area (8), the stagnation pressure region in front of the wing (9), and the low-pressure zone on the edge of the wheel arch to the left of the wheel center (10) show good agreement. The pressure distribution along the wheel arch, moving clockwise, is also comparable, although the exact positions of individual vortex footprints differ slightly between the measurement and simulation. Comparing these vortex footprints reveals that the separation zone around the air curtain (1) is more present in the experiment than in the simulation. Additionally, the separation caused by vortex (6) appears spatially lower in the experiment, and the footprint of vortex (7) is more distinct and extends further downward. These experimental findings on the wheel arch are supported by the wall pressure taps, which align with the PSP intensity gradients. On the disc, another difference between simulation and experiment is observed: while the footprint of vortex (4) is more prominent in the simulation, vortex (3) appears stronger in the experimental data. The origin of these discrepancies is currently unclear and will be the subject of future investigations.

This section focuses on pressure fluctuations to identify vortex footprints and their associated frequencies on the body and disc. As examples, Figure 11 a) shows a region on the body fluctuating at $36-37$ Hz, and Figure 11 b) shows a region on the disc fluctuating at $23-24$ Hz, demonstrating the setup's capability to detect such phenomena. At $36-37$ Hz, a separation is observed in the upper right area of the wheel arch, likely corresponding to vortex (5), assigning it this frequency. At $23-24$ Hz, a region of fluctuating pressure is found in the lower right area of the disc, presumably caused by reattachment of flow that separates at the lower front edge of the tire. Detailed evaluations of these phenomena will be addressed in future work.

The yellow areas in the outer body regions in both images (a + b) show a broadband camera noise across all frequencies due to the decrease in signal intensity towards the outer regions.

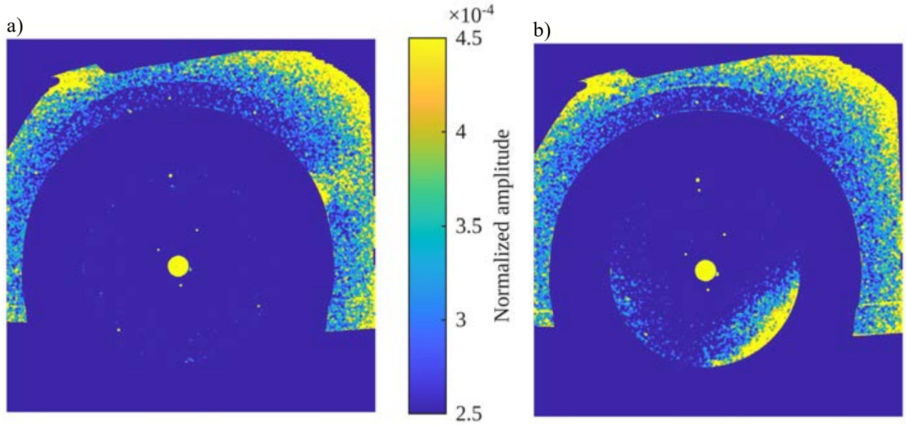

Figure 11: Frequency maps from the PSP measurements:
(a) $36 - 37$ Hz and b) $23 - 24$ Hz.

5 Summary and Outlook

This paper presents a measurement setup that enables the use of pressure-sensitive paint (PSP) to measure surface pressures on the rims of rotating wheels and adjacent body areas of a passenger car, both in wind tunnel and on-road tests. Furthermore, it includes initial evaluated principle measurements with stationary wheels, where a disc was mounted on the rim to simplify the geometry. The PSP was applied to this disc and the surrounding body surfaces.

In summary, the successful use of fast-response PSP in our setup was demonstrated, which opens new possibilities for spatially resolved, time-averaged, and unsteady surface pressure measurements. The accuracy of these initial principle tests was evaluated both qualitatively and quantitatively, with maximum deviations of 50 Pa between wall pressure taps and PSP measurements, which corresponds to $\Delta c_{\mathrm{p}} = \pm 0.05$ for dynamic pressures of approximately 930 Pa. It was shown that PSP can be used not only to measure averaged pressure fields but also to capture unsteady pressure fluctuations, allowing the assignment of frequencies to individual flow structures.

Future work will focus on measurements with rotating wheels to gain detailed insights into surface pressures on the rims and adjacent body areas, both averaged and time-resolved. Building on this, measurements will be conducted in both wind tunnel and road environments to identify, understand, and evaluate differences caused by ground simulation using five-belt systems. Furthermore, this promises high-quality data to further improve CFD simulations.

6 Reference list

[1] J. Hurlbrink, „Analyse der aerodynamischen Verlustmechanismen der Radhausströmung von Pkw und Entwicklung von Maßnahmen zur Luftwiderstandsreduktion,“ 2022.

[2] Krüger, L., Joksimovic, I., Wegt, S., Burgbacher, J. et al., “Influence of Wheel Wake on Vehicle Aerodynamics: An EddyResolving Simulation Study,” SAE Technical Paper 2023-01-0842, 2023, doi:10.4271/2023-01-0842.

[3] D. Möllenbeck, A. Fischer und H. Schmidt, „Impact of Wheel Drive Unit Secondary Flows on the Aerodynamics of Passenger Cars,“ (2024), In: Kulzer, A.C., Reuss, HC., Wagner, A. (eds) 2024 Stuttgart International Symposium on Automotive and Engine Technology. ISSYM 2024. Proceedings. Springer Vieweg, Wiesbaden. https://doi.org/10.1007/978-3-658-45018-2_3.

[4] E. Josefsson, M. Urquhart und S. Sebben, Influence of Wheel Drive Unit Belt Width on the Aerodynamics of Passenger Vehicles, SAE Technical Paper 2023-01-0657, 2023, https://doi.org/10.4271/2023-01-0657.

[5] M. Hilfer, M. Behn, C. Klein, T. Ahlefeldt, U. Tapken, L. Katzenmeier, L. Koop und L. Enghardt, „Near-field measurements of stationary and rotating in-duct sound sources with pressure sensitive paint,“ 2022, https://doi.org/10.2514/6.2022-3056.

[6] E. Duell, D. Everstine, R. Mehta, J. Bell und M. Perry, „Pressure-Sensitive Paint Technology Applied to Low-Speed Automotive Testing,“ SAE International, 2001.

[7] J. W. Gregory, H. Sakaue, T. Liu und J. P. Sullivan, „Fast Pressure-Sensitive Paint for Flow and Acoustic Diagnostics,“ Annual Review of Fluid Mechanics, 2014, doi: 10.1146/annurev-fluid-010313-141304.

[8] M. Kasai, A. Suzuki, Y. Egami, T. Nonomura und K. Asai, „A platinum-based fast-response pressure-sensitive paint containing hydrophobic titanium dioxide,“ Sensors and Actuators A: Physical, 2023, https://doi.org/10.1016/j.sna.2022.114140.

[9] A. Sieling, „Entwicklung einer Messmethode zur instationären Messung des Druckfeldes auf einer rotierenden Felge und dem angrenzenden Karosseriebereich im Windkanal- und Freifahrtversuch,“ 2025.

[10] TÜV NORD Mobilität GmbH und Co. KG, „Inspection of measuring and test equipment Aerodynamik-Aeroakustik-Kanal (AAK) at Volkswagen AG Wolfsburg,“ 2023.

[11] J. M. Hübner, M. Hähnel, S. Dr. Lange und M. Lemke, „Computational Method to Determine the Cooling Airflow Utilization Ratio of Passenger Cars Considering Component Deformation,“ SAE Technical Paper 2024-01-2975, 2024, doi:10.4271/2024-01-2975.